

Rapid quantification of clostridial epsilon toxin in complex food and biological matrices by immunopurification and ultra-performance liquid chromatography-tandem mass spectrometry

Alexandre SEYER¹, François FENAILLE¹, Cecile FERAUDET-TARISSE¹, Hervé VOLLAND¹, Michel R. POPOFF², Jean-Claude TABET³, Christophe JUNOT¹, François BECHER¹

* **To whom correspondence should be addressed.** Phone: 33-1-69-08-13-15. Fax: 33-1-69-08-59-07. E-mail: francois.becher@cea.fr

¹ **CEA**, iBiTec-S, Service de Pharmacologie et d'Immunoanalyse, 91191 Gif-sur-Yvette.

² **Institut Pasteur**, Unité des Bactéries Anaérobies et Toxines, 75724 Paris Cedex 15.

³ **Université Pierre et Marie Curie**, Laboratoire de Synthèse, Structure et Fonction de Molécules Bioactives, CNRS UMR 7613, 75252 Paris, France

Supplementary data

METHODS

Intact protein mass measurements and conditions of top-down experiments. Intact protein (1 mM in H₂O/AcN/FA 50:50:0.1 v:v:v) mass measurements and collision-induced dissociation (CID) MS/MS experiments were performed on a quadrupole time-of-flight (qTOF) mass spectrometer (maXis UHR qTOF MS, Bruker Daltonik, Bremen, Germany) fitted with a NanoMate (Advion Biosciences, Ithaca, NY, USA) nanoESI interface (3 μ L of sample per infusion). The instrument was controlled via Compass ver.1.3 (Bruker Daltonik) software package. It was operated at 1.5 Hz in the positive ion mode with an m/z range of 350-2000 in both MS and MS/MS mode. The drying temperature, nebuliser gas and drying gas were set at 180°C, 40 psi and 8 L/min, respectively. The isolation width was set at m/z 100, centred around the most intense ion, and the collision energy E_{lab} was 25 eV. Parent and product ions were transferred to the TOF analyser at the rate of 6 kHz and signal digitisation was performed at 4 GHz. MS and MS/MS data were deconvoluted with MaxEnt (Maximum Entropy, Data Analysis, Bruker Daltonik, Bremen, Germany). Resulting mass lists of product ions were searched against known sequences of epsilon protoxin and toxin proteins using Biotools software (Bruker Daltonik, Bremen, Germany). Manual inspection of each Biotools hit was performed by fitting raw data to theoretical y - and b -type fragment ions.

Bottom-up experiments. Epsilon protoxin and toxin were digested using the following method. Proteins (30 μ L at 1 mg.mL⁻¹ in 400 mM ammonium bicarbonate buffer pH 7.5) were incubated at 60°C for one hour with 8 M urea and 10 mM dithiothreitol. Samples were then placed for 45 min in a dark room at ambient temperature with iodoacetamide (10 μ L at 25 mM). To reduce the urea concentration before proteolysis, ammonium bicarbonate buffer was added (100 μ L at 400 mM). Trypsin (10 μ L at 100 μ g.mL⁻¹ in water) was finally added to samples and allowed to react at 37°C for 16 h. Digested epsilon protoxin and toxin were analysed by UPLC-ESI-MS/MS in the data-dependant acquisition mode in a LTQ-Orbitrap

instrument coupled with an Accela UHPLC system (Thermo Scientific, San Jose, CA). Peptides were eluted from a Zorbax 300 SB-C18 RRHD column (2.1 mm x 100 mm i.d., 300 Å porosity, 1.8 µM particle size, Agilent Technologies, Palo Alto, CA, U.S.A.) at 500 µL.min⁻¹ using a 5%-60% phase B gradient (phase A: 0.1% formic acid in ultrapure water, phase B: 0.1% formic acid in AcN) over 12 min. The source conditions were as follows: capillary temperature, 275°C; sheath gas flow, 80 arbitrary units; auxiliary gas flow, 20 arbitrary units; ESI spray voltage, 4.5 kV. The instrument was set up to automatically acquire full scan over the 300-2000 *m/z* range with a resolution set at 30000, followed by MS/MS spectra (with a normalised collision energy of 35% and an isolation width of 2.0 Th) of the three most intense ions. The ion population was set at 1.10⁶ in the Orbitrap in the full scan mode and at 1.10⁴ in the LTQ in MSn mode. Data analysis was performed both manually and using the Sequest algorithm included in the Bioworks Browser (Version 3.3.1 SP1, Thermo, San Jose, CA). MS and MS/MS spectra were searched against a restricted database consisting of the *C. perfringens* proteome. Alkylation of cysteine residues was defined as a fixed modification (+57.0215) and oxidation (15.9949), as a variable one. Finally, the number of missed cleavages was set at 0.

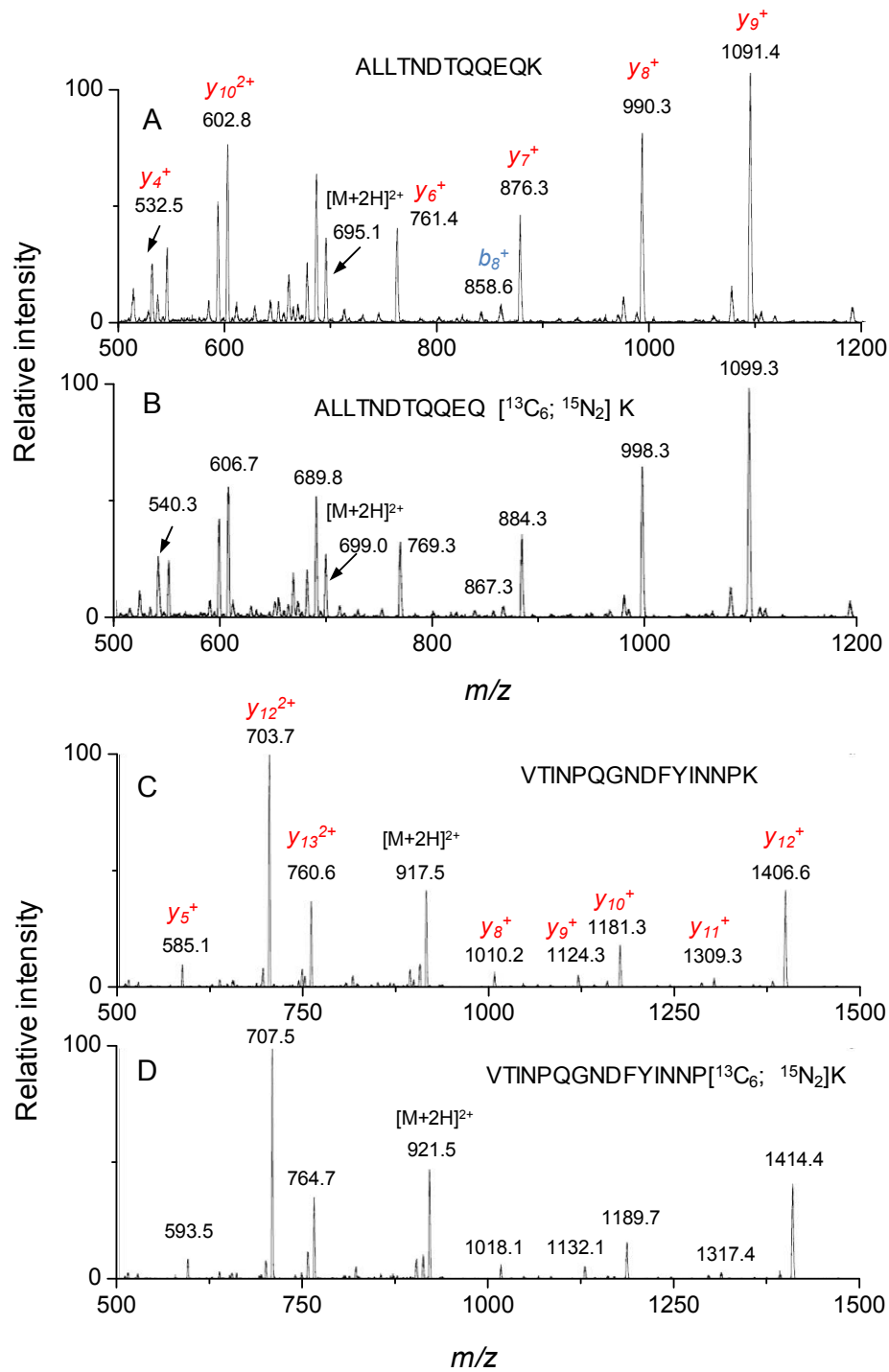


Figure S2. CID spectra of $[M+2H]^{2+}$ of peptides ALLTNDTQEQK (A; m/z 695.1; collision energy E_{lab} : 24 eV) and VTINPQGNDFYINNP (C; m/z 917.5; collision energy E_{lab} : 30 eV) along with their corresponding labelled homologue (B and D, respectively) recorded on a Xevo TQ MS in infusion mode.

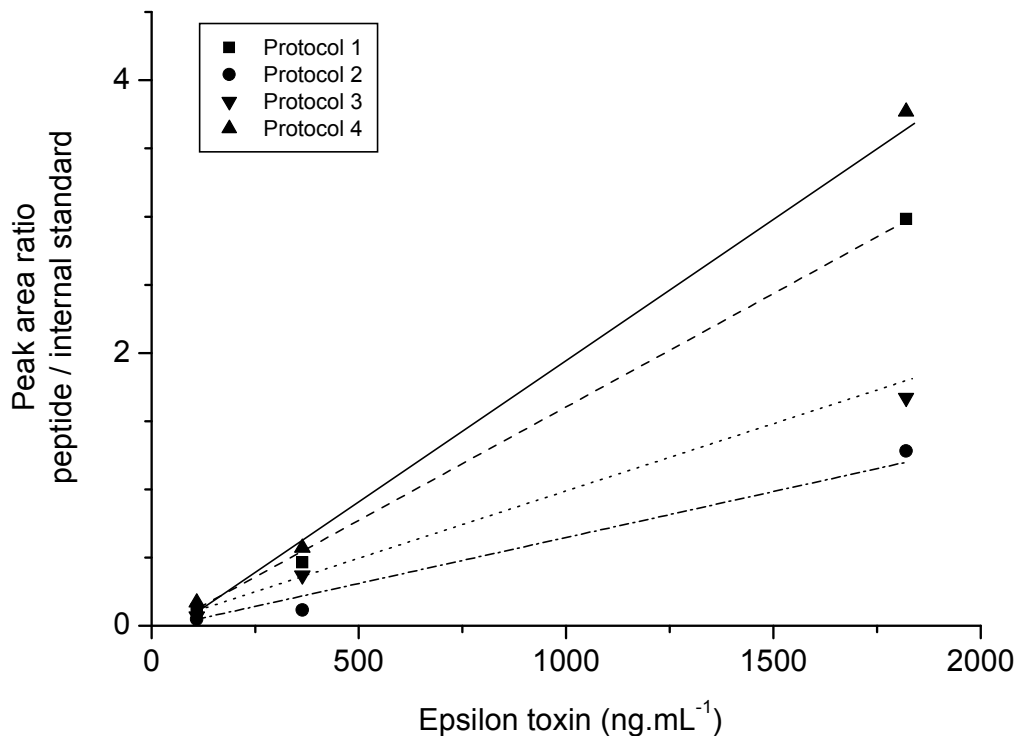


Figure S3. Comparison of four different denaturation methods, following the immunocapture of milk samples spiked with 100 ng.mL^{-1} , 350 ng.mL^{-1} and 1800 ng.mL^{-1} of epsilon toxin. **Protocol 1:** For protein denaturation, beads were resuspended in $30 \mu\text{L}$ of 8 M urea and incubated at 60°C for one hour. **Protocol 2:** Beads were resuspended in $30 \mu\text{L}$ of 400 mM ammonium bicarbonate buffer ($\text{NH}_4(\text{HCO}_3)$) and incubated at 60°C for one hour with dithiothreitol ($10 \mu\text{L}$ at 10 mM) and for 45 min in a dark room with iodoacetamide ($10 \mu\text{L}$ at 25 mM). **Protocol 3:** Beads were resuspended in $150 \mu\text{L}$ of $\text{NH}_4(\text{HCO}_3)$ $400 \text{ mM}/\text{AcN}$ $20:80$ v:v and incubated at 95°C for 5 min. AcN was evaporated after digestion. **Protocol 4:** Beads were resuspended in $30 \mu\text{L}$ of 0.05% RapidGest SF (in 400 mM $\text{NH}_4(\text{HCO}_3)$) and incubated for 10 min at 95°C . After protein denaturation, trypsin was added ($5 \mu\text{L}$ at $100 \mu\text{g.mL}^{-1}$ in water) and samples were incubated at 37°C for 16 h. Finally, to maintain a final volume of $100 \mu\text{L}$ for each sample, the required volume of $\text{H}_2\text{O}/\text{AcN}/\text{formic acid}$ $95:5:0.1$ v:v:v was added along with the internal standard (50 ng.mL^{-1}).

The y axis corresponds to the area ratio of the MRM transition m/z 917.5 to m/z 703.7 (peptide VTINPQGNDFYINNPk) with the corresponding internal standard. Two independent analyses were performed for each concentration.

These experiments were performed using an HP 1100 HPLC system from Agilent Technology (Palo Alto, CA, U.S.A.) coupled to a triple-quadrupole TSQ Quantum Ultra mass spectrometer (Thermo Scientific, San Jose, CA, U.S.A.). Chromatographic separation was performed on a Zorbax SB-C18 column (150 mm x 2.1 mm i.d., 5 μ m particle size, 300 Å porosity) from Agilent Technology (Palo Alto, CA, U.S.A.).

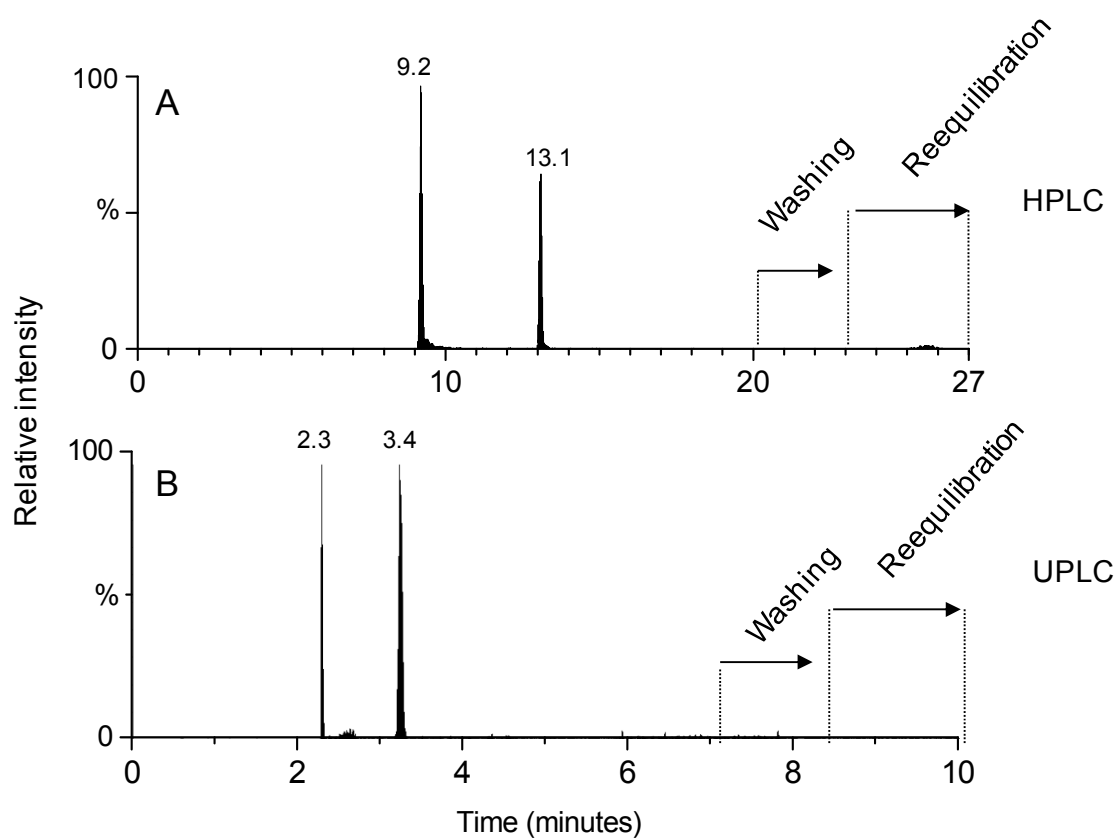


Figure S4. MRM chromatograms of the two peptides used for quantification after immunocapture and proteolysis of epsilon toxin spiked in milk and analysed by HPLC (A) and by UPLC (B) systems. Two different mass spectrometers were used. Peaks at 9.2 min (HPLC) and 2.3 min (UPLC) correspond to the peptide ALLTNDTQQEQK and peaks at 13.1 min (HPLC) and 3.4 min (UPLC) correspond to the peptide VTINPQGNDFYINNPk.

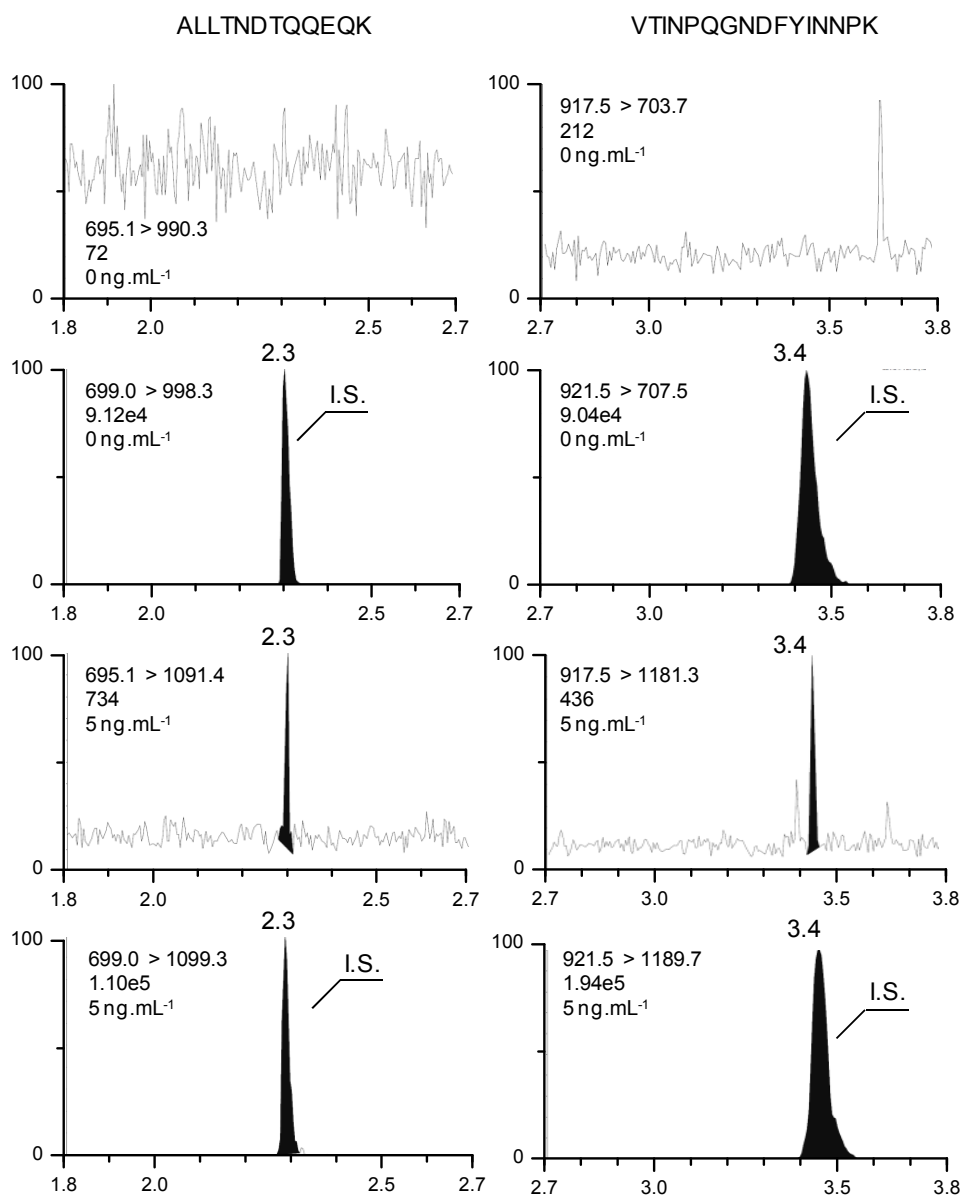


Figure S5. UPLC-MS/MS chromatograms of one MRM transition of each peptide at 0 ng.mL⁻¹ and 5 ng.mL⁻¹ in milk with their respective internal standard.

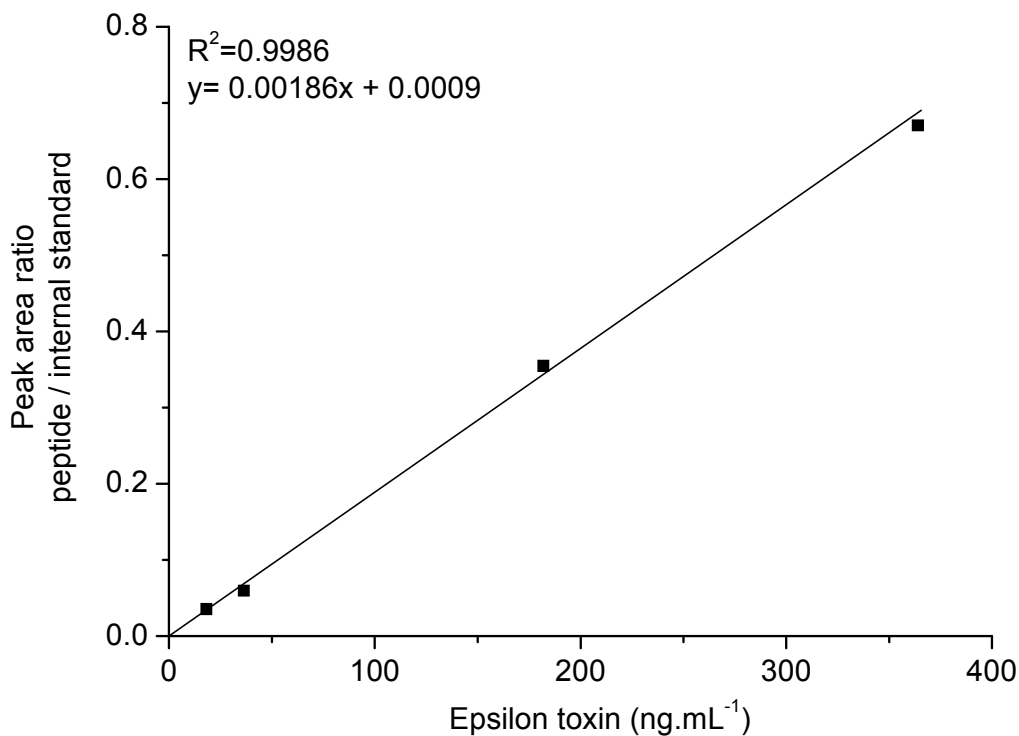


Figure S6. Calibration curve of epsilon toxin spiked in serum from 5 ng.mL⁻¹ to 350 ng.mL⁻¹. Calibration was done by fitting a linear regression of the area of the MRM transition m/z 917.5 to m/z 703.7, peptide VTINPQGNDFYINNPk, with the corresponding internal standard again epsilon toxin concentration. Two independent analyses were performed for each concentration.

These experiments were performed using an HP 1100 HPLC system from Agilent Technology (Palo Alto, CA, U.S.A.) coupled to a triple-quadrupole TSQ Quantum Ultra mass spectrometer (Thermo Scientific, San Jose, CA, U.S.A.). Chromatographic separation was performed on a Zorbax SB-C18 column (150 mm x 2.1 mm i.d., 5 μ m particle size, 300 Å porosity) from Agilent Technology (Palo Alto, CA, U.S.A.).

Table S1. Fragment ions obtained by MS/MS experiments under CID conditions for the epsilon toxin and prototoxin species with their respective *m/z* ratio deviation.

N-terminal sequences	<i>b</i> -type fragments	Average deviation (ppm)
Epsilon toxin		
KEISNTVSNEMSKKASYDNVDTL [...]	$b_{55}^{8+}, b_{57}^{10+}$	5.8
VSNEMSKKASYDNVDTL [...]	$b_9^{1+}, b_{42}^{7+}, b_{42}^{8+}, b_{50}^{6+}, b_{50}^{7+}, b_{50}^{8+}, b_{50}^{9+}, b_{50}^{10+}, b_{58}^{7+}, b_{58}^{8+}, b_{58}^{9+}, b_{68}^{7+}, b_{68}^{8+}, b_{68}^{9+}, b_{68}^{10+}, b_{68}^{11+}, b_{68}^{12+}, b_{68}^{13+}$	6.2
KASYDNVDTL [...]	$b_{35}^{5+}, b_{35}^{6+}, b_{42}^{6+}, b_{42}^{7+}, b_{43}^{5+}, b_{43}^{7+}, b_{43}^{8+}, b_{44}^{7+}, b_{44}^{8+}, b_{44}^{9+}, b_{45}^{6+}, b_{45}^{7+}, b_{45}^{8+}, b_{45}^{9+}, b_{48}^{5+}, b_{48}^{6+}, b_{48}^{7+}, b_{48}^{8+}, b_{48}^{9+}, b_{48}^{10+}, b_{52}^{6+}, b_{52}^{7+}$	5.5
Epsilon prototoxin		
KEISNTVSNEMSKKASYDNVDTL [...]	$b_6^{1+}, b_{49}^{5+}, b_{49}^{6+}, b_{53}^{7+}, b_{53}^{8+}, b_{63}^{6+}, b_{63}^{7+}, b_{63}^{8+}, b_{63}^{9+}, b_{67}^{7+}$	3.9
VSNEMSKKASYDNVDTL [...]	$b_{37}^{7+}, b_{39}^{8+}, b_{40}^{6+}, b_{40}^{7+}, b_{40}^{8+}, b_{41}^{7+}, b_{42}^{8+}, b_{42}^{5+}, b_{42}^{6+}, b_{42}^{7+}, b_{42}^{8+}, b_{42}^{9+}, b_{48}^{5+}, b_{48}^{6+}, b_{48}^{7+}, b_{48}^{8+}, b_{48}^{9+}, b_{49}^{5+}, b_{49}^{6+}, b_{49}^{7+}, b_{49}^{8+}, b_{49}^{9+}, b_{51}^{8+}, b_{51}^{10+}, b_{52}^{6+}, b_{52}^{7+}, b_{52}^{8+}, b_{52}^{9+}, b_{52}^{10+}, b_{55}^{5+}, b_{55}^{6+}, b_{55}^{7+}, b_{55}^{8+}, b_{55}^{9+}, b_{55}^{10+}, b_{56}^{5+}, b_{56}^{6+}, b_{56}^{7+}, b_{56}^{8+}, b_{56}^{9+}, b_{56}^{10+}, b_{58}^{6+}, b_{58}^{7+}, b_{58}^{8+}, b_{58}^{9+}, b_{64}^{6+}, b_{64}^{7+}, b_{68}^{6+}, b_{68}^{7+}, b_{68}^{8+}, b_{68}^{9+}, b_{68}^{10+}, b_{68}^{11+}, b_{68}^{12+}, b_{70}^{10+}, b_{70}^{11+}, b_{70}^{12+}, b_{87}^{9+}$	4.1
KASYDNVDTL [...]	$b_{43}^{5+}, b_{43}^{6+}, b_{64}^{11+}, b_{64}^{12+}, b_{127}^{19+}$	5.4
C-terminal sequences	<i>y</i> -type fragments	Average deviation (ppm)
Epsilon toxin		
[...] VQEYVIPVDKK	$Y_{26}^{4+}, Y_{39}^{5+}, Y_{39}^{6+}, Y_{39}^{7+}, Y_{42}^{6+}, Y_{68}^{7+}, Y_{68}^{8+}, Y_{68}^{9+}, Y_{68}^{10+}, Y_{68}^{11+}, Y_{70}^{10+}, Y_{70}^{11+}$	4.8
[...] VQEYVIPVDK	$Y_{40}^{5+}, Y_{40}^{6+}, Y_{67}^{6+}, Y_{67}^{7+}, Y_{67}^{8+}, Y_{67}^{9+}, Y_{69}^{7+}, Y_{69}^{8+}, Y_{69}^{9+}, Y_{74}^{10+}, Y_{104}^{11+}$	6.7
Epsilon prototoxin		
[...] VQEYVIPVDKKEKSNDSNIVKYRSLSIKAPGIK	$Y_{24}^{3+}, Y_{24}^{4+}, Y_{27}^{4+}, Y_{27}^{5+}, Y_{27}^{6+}, Y_{29}^{3+}, Y_{29}^{4+}, Y_{29}^{5+}, Y_{29}^{6+}, Y_{29}^{7+}, Y_{29}^{8+}, Y_{30}^{4+}, Y_{30}^{5+}, Y_{30}^{6+}, Y_{30}^{7+}, Y_{31}^{3+}, Y_{31}^{4+}, Y_{31}^{5+}, Y_{31}^{6+}, Y_{31}^{7+}, Y_{31}^{8+}, Y_{32}^{5+}, Y_{32}^{6+}, Y_{32}^{7+}, Y_{33}^{7+}, Y_{33}^{8+}, Y_{34}^{9+}, Y_{34}^{10+}, Y_{48}^{9+}, Y_{48}^{10+}, Y_{48}^{11+}, Y_{48}^{12+}, Y_{49}^{7+}, Y_{49}^{8+}, Y_{49}^{9+}, Y_{49}^{10+}, Y_{63}^{9+}, Y_{63}^{10+}, Y_{63}^{11+}, Y_{63}^{12+}$	3.7
[...] VQEYVIPVDK	$Y_{67}^{6+}, Y_{67}^{7+}, Y_{67}^{8+}, Y_{67}^{9+}$	5.6

Table S2. Tryptic peptides observed for epsilon toxin and prototoxin by LC-MS/MS experiments.

Position	Sequence	Experimental monoisotopic masses [M+H] ⁺ after deconvolution	Error (ppm)
Epsilon prototoxin			
34-45	EISNTVSNEMSK	1338.62	1.3
47-58	ASYDNVDTLIEK	1367.67	0.7
65-69	YNYLK	700.36	4.8
74-84	YYPNAMAYFDK	1382.61	1.0
85-100	VTINPQGNDFYINNP	1833.91	4.3
101-119	VELDGEPSMNYLEDVYVGK	2157.00	0.9
120-131	ALLTNDTQQEQK	1388.70	0.7
134-140	SQSFTCK	857.38	4.3
135-162	NTDVTATTTHTVGTSIQATAK	2219.11	1.0
163-190	FTVPFNETGVSLTTSYFANTNTNTNSK	3042.41	7.4
191-216	EITHNVPSQDILVPANTTVEVIAYLK	2864.54	1.7
218-221	VNVK	459.29	0.6
222-225	GNVK	417.24	4.4
226-246	LVGQVSGSEWGEIPSYLAFPR	2292.16	0.7
247-250	DGYK	482.22	4.2
251-259	FSLSDTVNK	1495.74	0.9
260-273	SDLNEDGTININGK	1489.71	3.7
274-287	GNYSAVMGDELIVK	1495.74	1.1
290-305	NLNTNNVQEYVIPVDK	1859.94	4.2
309-316	SNDSNIVK	876.44	5.0
319-323	SLSIK	338.18	3.2
324-328	APGIK	547.34	4.1
Epsilon toxin			
34-45	EISNTVSNEMSK	1338.62	1.9
47-58	ASYDNVDTLIEK	1367.67	1.3
65-69	YNYLK	700.36	4.6
74-84	YYPNAMAYFDK	1382.61	1.1
85-100	VTINPQGNDFYINNP	1833.91	4.2
101-119	VELDGEPSMNYLEDVYVGK	2157.00	0.3
120-131	ALLTNDTQQEQK	1388.70	2.4
134-140	SQSFTCK	857.38	3.6
135-162	NTDVTATTTHTVGTSIQATAK	2219.11	0.2
163-190	FTVPFNETGVSLTTSYFANTNTNTNSK	3042.42	5.4
191-216	EITHNVPSQDILVPANTTVEVIAYLK	2864.53	2.1
218-221	VNVK	459.29	0.6
222-225	GNVK	417.24	4.4
226-246	LVGQVSGSEWGEIPSYLAFPR	2292.16	0.4
247-250	DGYK	482.22	4.3
251-259	FSLSDTVNK	1495.75	0.7
260-273	SDLNEDGTININGK	1489.71	1.9
274-287	GNYSAVMGDELIVK	876.44	4.1
290-305	NLNTNNVQEYVIPVDK	1859.94	3.6
319-323	SLSIK	547.34	4.7
324-328	APGIK	485.31	5.3

Table S3. Accuracy of samples spiked with three different quantities of epsilon toxin or prototoxin against a toxin calibration curve for the MRM transition m/z 917.5 to m/z 703.7 (peptide VTINPQGNDFYINNPk).

Epsilon toxin			Epsilon prototoxin		
Theoretical concentration (ng.mL ⁻¹)	Measured concentration (ng.mL ⁻¹)	Accuracy (%)	Theoretical concentration (ng.mL ⁻¹)	Measured concentration (ng.mL ⁻¹)	Accuracy (%)
18.2	16.4	90.2	19.3	14.7	76.2
91.0	99.1	108.9	96.3	71.3	74.0
364.0	364.3	100.1	385.0	273.3	71.0